Fechner, D.; Hort, N.; Blawert, C.; Dieringa, H.; Stoermer, M.; Kainer, K.U.:

The Formation of Sr6.33Mg16.67Si13 in Magnesium Alloy AM50 and its Effect on Mechanical Properties

In: Journal of Materials Science (2012) Springer

DOI: 10.1007/s10853-012-6436-9

The Formation of $Sr_{6.33}Mg_{16.67}Si_{13}$ in Magnesium Alloy AM50 and its Effect on Mechanical Properties

Daniel Fechner [a, b], Norbert Hort [a], Carsten Blawert [a], Hajo Dieringa [a], Michael Störmer [c], Karl Ulrich Kainer [a]

[a] *Magnesium Innovation Centre MagIC, Institute of Materials Research, Helmholtz-Zentrum Geesthacht, Max-Planck-Straße 1, 21502 Geesthacht, Germany*

[b] *corresponding author, present affiliation:*
Competence Centre Material and Welding Technology, Technikzentrum, TÜV-NORD Systems GmbH & Co. KG,
Große Bahnstaße 31, 22525 Hamburg, Germany,

phone: +49(0)4085571097,

fax: +49(0)4085572710,

e-mail: dfechner@tuev-nord.de

[c] *Materials Technology, Institute of Materials Research, Helmholtz-Zentrum Geesthacht, Max-Planck-Straße 1, 21502 Geesthacht, Germany*

Abstract

The increasing use of magnesium castings for automotive components and the number of newly developed alloys raise the question of suitable recycling processes. Remelting offers a high potential of energy saving and thereby improves the live cycle balance of magnesium components. Effective recycling processes are likely to involve the mixing of different alloys but little is known about the interaction of alloying elements. In order to approach this issue, the influence of strontium, silicon and calcium on phase formation and mechanical properties of magnesium alloy AM50 has been investigated. After strontium addition, X-ray diffraction demonstrated the formation of the Al_4Sr- and the $Mg_{17}Sr_2$-phase. However, after simultaneous alloying with strontium, silicon and calcium the ternary Zintl-phase $Sr_{6.33}Mg_{16.67}Si_{13}$ was detected. This phase forms preferably instead of Al_4Sr, $Mg_{17}Sr_2$ and Mg_2Si. Compared to the two strontium-containing phases, precipitates of the ternary Zintl-phase exhibit a rather compact morphology. This results in a higher elongation-at-fracture under tensile stress.

Keywords: magnesium alloys, recycling, silicon, strontium, calcium, Zintl-phase

Introduction

Magnesium primary production has been growing considerably within the last 15 years [1-3]. About half of the world production is used for alloy fabrication and the alloys are predominantly used in the automotive sector. Lightweight construction can reduce CO_2 emissions of combustion engines driven vehicles and enlarge the cruising range of upcoming electric vehicles. With the invention of several cost competitive, heat resistant high pressure die casting alloys, the variety of commercial magnesium materials for automotive applications has been considerably broadened. This allowed the fabrication of an increasing number of magnesium drive train components like gearbox housings and crankcases [4,5].

Due to the above mentioned circumstances, an increasing use of magnesium for automotive components is probable. This will cause a rising quantity of magnesium scrap from end-of-life vehicles, ELV, in the future. Magnesium recycling by means of remelting so far is only practiced for clean scrap sorted according to one alloy composition. For recycling of ELV the shredder process is most commonly used today and due to economic reasons this is likely to be so in future [6]. Shredding inevitably causes the intermixture of different magnesium alloys and so this scrap today is not used for alloy fabrication. For aluminium it is common practice to use mixed scrap from different alloys to produce new aluminium materials [7]

Research on magnesium-recycling alloys has been performed for the most common magnesium-aluminium-zinc-system, also AZ-system, and the magnesium-aluminium-manganese-system, also AM-system [8-10]. The most important cost competitive, heat resistant alloys are based on the AM-system, with the alloying elements strontium, silicon and calcium ensuring thermal stability. No concepts are available to handle the input of these alloying elements into magnesium scrap from ELV. However, components of these materials are in use for vehicles of different car manufacturers and a corresponding high quantity of scrap can be expected.

Strontium, silicon and calcium form characteristic phases in the above mentioned heat resistant materials. In magnesium-aluminium-strontium alloys like AJ52A and AJ62A, the Al_4Sr- and $Mg_{17}Sr_2$-phases are present [11,12]. Materials from the so called AJ-system contain between 1.7 % and 2.8 % of strontium [13]. The binary Zintl-phase Mg_2Si is characteristic for magnesium-aluminium-silicon alloys like AS31 [4]. Alloys of the AS-system contain between 0.5 % and 1.5 % of silicon [13]. Al_2Ca is the phase frequently associated with magnesium-aluminium-calcium alloys like MRI153M and MRI230D [14,15]. AX-alloys contain 1 % to 2.5 % calcium. Strontium- and calcium-containing phases in the above mentioned alloys incorporate aluminium and suppress the formation of the $Mg_{17}Al_{12}$-phase. The occurrence of $Mg_{17}Al_{12}$ generally reduces the creep resistance of magnesium alloys [16,17]. Silicon does not react with aluminium but Mg_2Si is said to stabilise grain boundaries [18]. Besides, alloys of the AS-system usually contain less aluminium and therefore exhibit a lower content of $Mg_{17}Al_{12}$-phase.

The commercial AJ-, AS- and AX-systems have been investigated thoroughly but the simultaneous addition of the three main alloying elements has not been studied this far. However, the latter is crucial if the idea of magnesium recycling by remelting scrap from ELV is to be considered. Two similarities can be seen in the chemical composition of cost competitive, heat resistant magnesium alloys. They contain about 0.3 % manganese and between 1.8 % to 8.4 % aluminium. The high pressure die casting alloy AM50 with a manganese content of 0.3 % and an aluminium content of 5.0 % comprises these two similarities. Therefore AM50 was chosen as the base alloy for the experiments.

Within a dissertation [19-22], a matrix of potential magnesium recycling alloys was set up with the alloy AM50 as the base material. Different quantities of strontium, silicon and calcium were added to simulate the composition of upcoming scrap material. All alloys were prepared by permanent mould casting. The alloys were based on alloy AM50 and contained varying additions of strontium, silicon and calcium. This article describes the preparation of eight alloys, which were selected due to their phase formation. The materials were investigated for their microstructure, their tensile properties and their creep resistance under compressive loads.

Experimental

Tab. 1 shows the intended composition of the prepared alloys. Calcium- and silicon contents are indicated on the left hand side of the table, strontium contents are indicated together with the names of the alloys. For alloy preparation, sectioned ingots of AM50 alloy were molten at 730 °C. The alloying elements were added in their pure form. After 30 minutes of stirring and 15 minutes of settling, the melt was poured into a permanent steel mould preheated to 400 °C. Ceramic foam filters, type Sivex FC, were supplied by company FOSECO. The filters were 50 mm x 50 mm x 22 mm in size. They were used in order to slow down the melt before passing through the gate and avoid air entrapments. The castings were 40 mm x 100 mm x 200 mm in size. A mixture of argon and 0.2 vol. % SF_6 was used to prevent melt oxidation.

The chemical composition was investigated using optical emission spectroscopy (OES). Microstructural investigations and phase analysis were performed by optical microscopy and X-ray diffraction. For XRD investigations a diffractometer with Cu-anode was used. The acceleration voltage was adjusted to 40 kV and the cathode current to 30 mA. The step size was set to 0.05 ° with a measuring time of 8 s per step. For metallographic preparation the samples were ground with silicon carbide paper down to 2500 grid and subsequently polished using an acid free oxide suspension. Etching was done in a mixture of ethanol, picric acid, glacial acetic acid and distilled water. After etching the samples were cleaned with ethanol and dried. Optical microscopy was performed with a microscope LEICA DMI5000M. For the determination of the grain size the linear intercept method according to ASTM standard E 112 – 96 [23] was applied. For each alloy the grain diameter was measured at two representative positions in the casting and three micrographs were evaluated for each position.

Tensile tests were performed according to standard DIN EN 10002-1 [24]. Round tensile test specimens were machined by turning according to standard DIN 50125 [25]. A tensile testing machine from company Zwick type Z050 was used. The elongation was measured using an extensometer. For compression creep tests round cylindrical specimens with a diameter of 6 mm and a length of 15 mm were machined by turning. The machines lever arm testers from company ATS Applied Test Systems. The elongation was measured using an extensometer. The temperature was measured by three thermocouples in the oven room and the accuracy of the temperature control was ± 3 °C. Creep tests were carried out for 200 h at 80 MPa and 150 °C Minimum creep rates were calculated from the last ten hours of the tests. All tensile tests and creep tests were repeated three times and the deviations are indicated in the corresponding graphs.

Results

Casting the alloys did not cause major problems except for materials containing 1 % silicon. The filters were sometimes blocked by undissolved particles of alloying elements and the solidified blocks suffered from shrinkage pores. Extra castings had to be prepared in order to receive enough material for sample preparation. Tab. 2 shows the chemical compositions of the selected materials. From alloy AM50 to AJM52 the strontium content has been subsequently raised while the levels of silicon and calcium remained unchanged. From alloy ASMX51 to AJSMX521 the same amounts of strontium have been added. The levels of silicon and calcium were increased to 1.0 wt.-% and 0.2 wt.-%, respectively, compared to the alloys AM50 to AJM52.

Tab. 1: Nominal chemical composition of permanent mould cast alloys based on alloy AM50 in wt.-%

Subsystem	**Strontium Content in wt.-% / Alloy Codification According to [26]**			
AM50	0 / AM50	0.5 / AJM50	1.0 / AJM51	2.0 / AJM52
AM50 + 0.2 Ca + 1.0 Si	0 / ASMX50	0.5 / ASJMX50	1.0 / AJSMX511	2.0 / AJSMX521

Tab. 2: Chemical composition of the permanent mould cast alloys in wt.-%, Mg remainder

Alloys	**Al**	**Mn**	**Sr**	**Si**	**Ca**	**Zn**	**Cu**	**Fe**	**Ni**
AM50	4.97	0.30	0.00	0.02	0.00	0.01	0.0005	0.0023	0.0008
AJM50	5.09	0.32	0.22	0.02	0.00	0.01	0.0006	0.0020	0.0006
AJM51	5.07	0.31	0.94	0.02	0.00	0.01	0.0006	0.0024	0.0008
AJM52	5.18	0.34	1.87	0.02	0.00	0.01	0.0007	0.0028	0.0006
ASMX51	4.92	0.30	0.00	1.05	0.13	0.01	0.0006	0.0027	0.0005
ASJMX51	5.21	0.28	0.51	1.11	0.13	0.01	0.0006	0.0013	0.0005
AJSMX511	5.17	0.26	0.80	0.93	0.13	0.01	0.0006	0.0020	0.0005
AJSMX521	5.12	0.32	1.98	1.14	0.14	0.01	0.0007	0.0029	0.0005

Fig. 1 shows the XRD patterns of alloys AM50 to AJM52. In the base alloy AM50 the α-matrix, Mg, and the $Mg_{17}Al_{12}$-phase, are the main constituents of the microstructure. Peaks of the Al_4Sr-phase increase steadily with the strontium content from alloy AJM50

to AJM52. The $Mg_{17}Al_{12}$–phase is detected up to an addition of 0.22 wt.-% strontium. Phase $Mg_{17}Sr_2$ with aluminium in solid solution [12] is present only in alloy AJM52. Comparisons of XRD patterns and light microscopic pictures shown in Fig. 2-Fig. 4 allow the optical identification of $Mg_{17}Al_{12}$ precipitates and the two strontium-containing phases. The $Mg_{17}Al_{12}$–phase can still be observed in the micrograph of alloy AJM51 containing 0.94 % strontium, see Fig. 3.

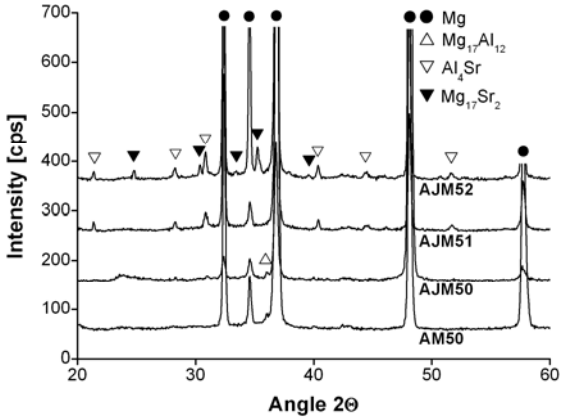

Fig. 1: XRD patterns of alloys without extra silicon

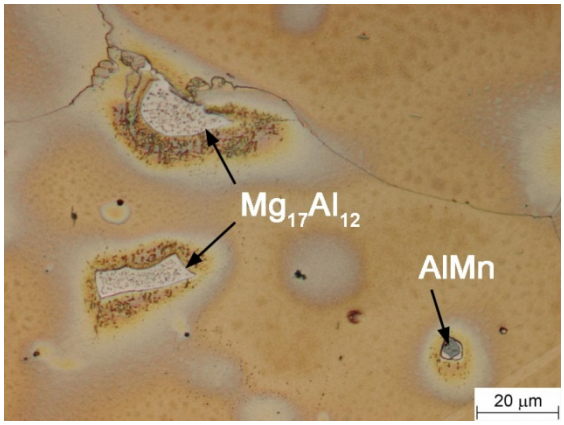

Fig. 2: Microstructure of alloy AM50

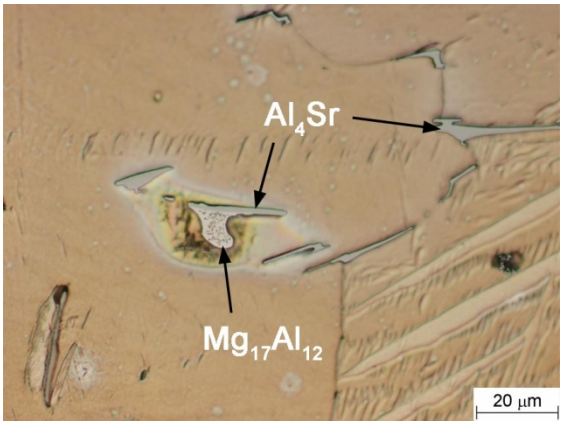

Fig. 3: Microstructure of alloy AJM51

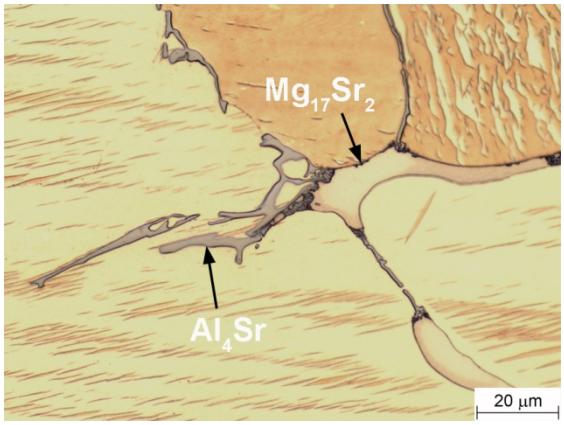

Fig. 4: Microstructure of alloy AJM52

Fig. 5 shows the XRD patterns of the alloys with 1 wt.-% silicon. The $Mg_{17}Al_{12}$–phase is found in all four materials. In alloy ASMX51 the Mg_2Si-phase is the only kind of precipitate apart from $Mg_{17}Al_{12}$ and the α–matrix. After the addition of strontium, the ternary Zintl-phase $Sr_{6.33}Mg_{16.67}Si_{13}$ is verified additionally. With an increasing amount of strontium, the peak heights of Mg_2Si decrease from alloy ASMX51 to AJSMX511. After addition of 2 wt.-% strontium the Mg_2Si-phase was not detected in AJSMX521 anymore. Instead the ternary Zintl-phase $Sr_{6.33}Mg_{16.67}Si_{13}$ and the Al_4Sr-phase are verified. The XRD pattern in Fig. 5 and a comparison between the microstructures in Fig. 2, Fig. 4 and Fig. 6 allow identification of the $Sr_{6.33}Mg_{16.67}Si_{13}$-phase. The precipitates exhibited a rather compact shape.

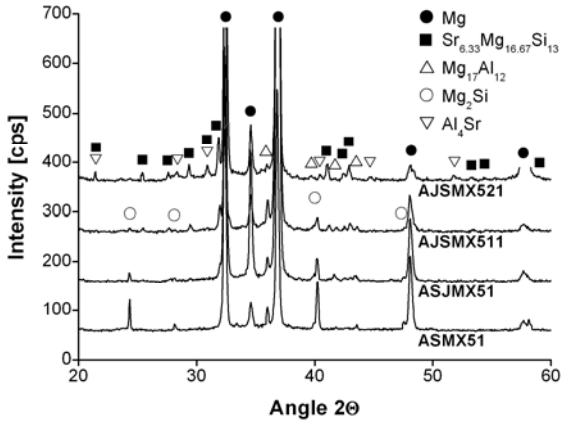

Fig. 5: XRD patterns of alloys with 1 % silicon

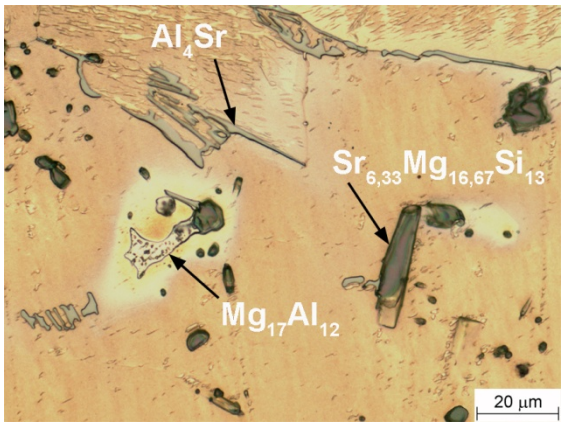

Fig. 6: Microstructure of alloy AJSMX521

In Tab. 3 the grain diameters of the alloys are presented. It can be seen that by trend the grain size is reduced with an increasing content of alloying elements. However a clear development is not observable.

Tab. 3: Grain diameters of the permanent mould cast alloys

Alloys	Grain diameter [mm]	Alloys	Grain diameter [mm]
AM50	519 ± 60	**ASMX51**	551 ± 44
AJM50	508 ± 18	**ASJMX51**	340 ± 57
AJM51	237 ± 31	**AJSMX511**	504 ± 51
AJM52	272 ± 20	**AJSMX521**	331 ± 48

Fig. 7-Fig. 9 show yield strength, ultimate tensile strength and elongation-at-fracture of all eight permanent mould cast alloys. Obviously the yield strength is improved by the rising content of strontium in the alloys without silicon addition. The elevated content of silicon also has a strengthening effect. The ultimate tensile strength is linked with the elongation-at-fracture as no necking occurred during the tests. It can be seen that the addition of alloying elements strongly reduced the elongation-at-fracture and therewith the ultimate tensile strength. However, it is noticeable that for materials without extra silicon the elongation at fracture is further reduced with a rising content of strontium, whereas the value remains more or less constant for alloys containing 1 % of silicon.

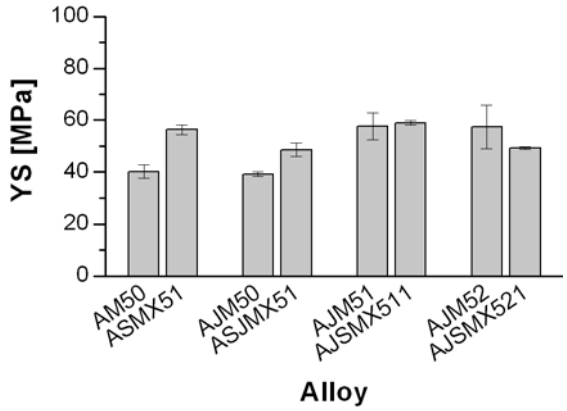

Fig. 7: Yield strength of the alloys

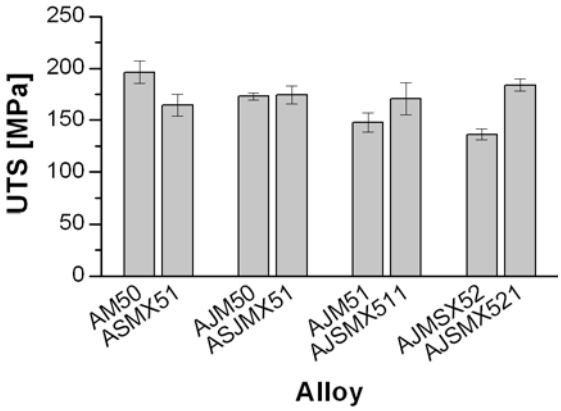

Fig. 8: Ultimate tensile strength of the alloys

Fig. 10 shows the minimum creep rates and the compressions measured during compression creep tests. Rising strontium-additions reduce the minimum creep rate as well as the plastic deformation of the samples. The same holds for alloys containing 1 % of silicon and 0.2 % calcium. For alloys with less than 1 % of strontium the silicon- and calcium-containing materials exhibit the lower minimum creep rate. For alloys with 1 % of strontium or more the opposite is true.

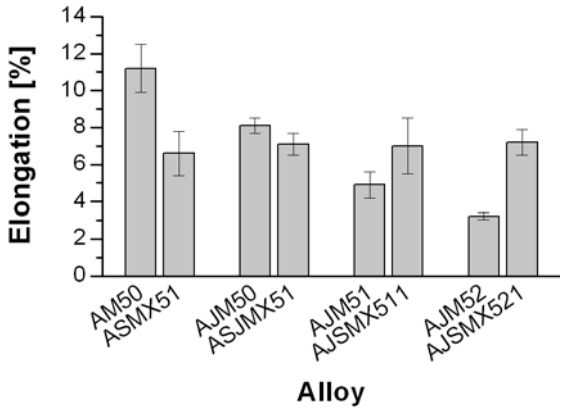

Fig. 9: Elongation-at-fracture of the alloys

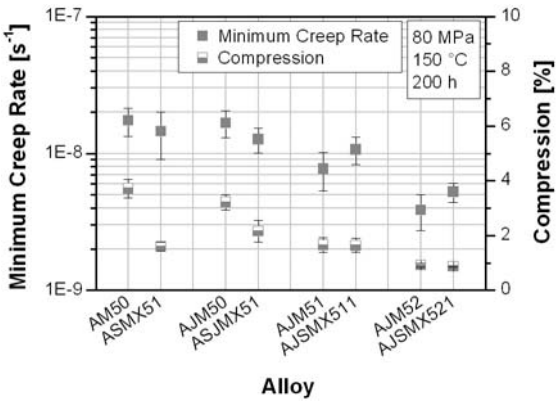

Fig. 10: Minimum creep rate of the alloys, compression creep

Fig. 11-Fig. 14 show the micrographs of fractured tensile samples from alloy AJM52 and AJSMX521. The white arrows indicate the former direction of the tensile stress. It can be seen that the phases Al_4Sr, $Mg_{17}Sr_2$ and $Sr_{6.33}Mg_{16.67}Si_{13}$ all show brittle fracture behaviour while cracks are frequently stopped in the magnesium-matrix. The phases Al_4Sr and $Mg_{17}Sr_2$ have a wide spread morphology compared to a rather compact appearance of $Sr_{6.33}Mg_{16.67}Si_{13}$ precipitates.

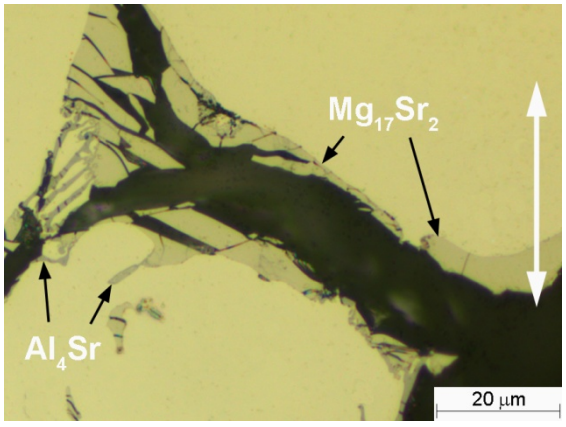

Fig. 11: Microstructure of fractured tensile specimen from alloy AJM52 with $Mg_{17}Sr_2$ and Al_4Sr precipitates

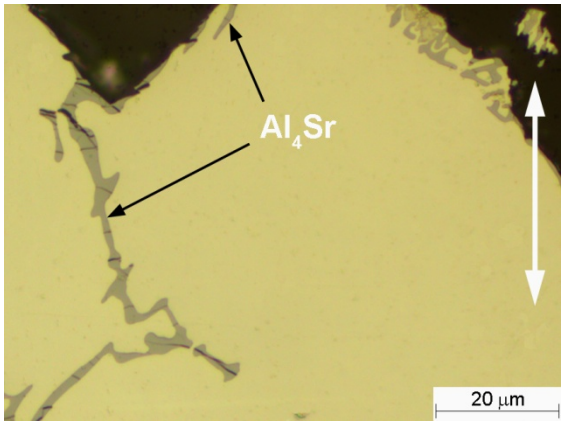

Fig. 12: Microstructure of fractured tensile specimen from alloy AJM52 with Al_4Sr precipitates

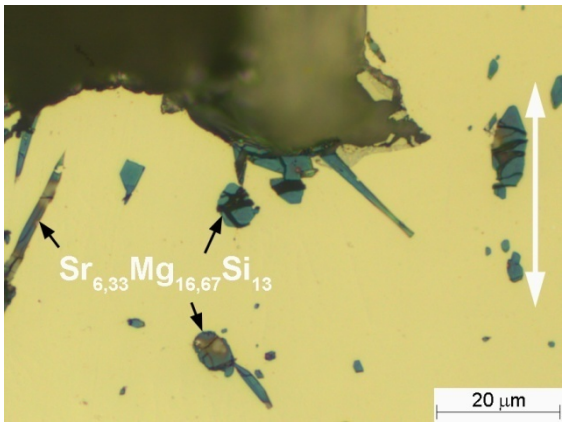

Fig. 13: Microstructure of fractured tensile specimen from alloy AJSMX521 with $Sr_{6.33}Mg_{16.67}Si_{13}$ precipitates

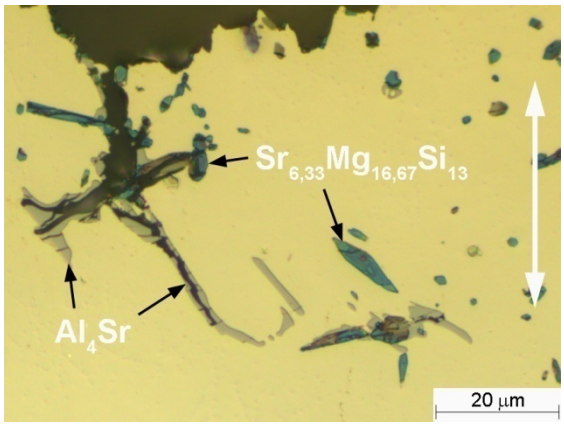

Fig. 14: Microstructure of fractured tensile specimen from alloy AJSMX521 with $Sr_{6.33}Mg_{16.67}Si_{13}$ and Al_4Sr precipitates

Discussion

The phase formations of alloy AM50 have been reported and the detection of the $Mg_{17}Al_{12}$-phase is in accordance with literature [27,28]. Al_4Sr and $Mg_{17}Sr_2$ are common precipitates in the AJ alloy system [11,12]. The formation of $Mg_{17}Sr_2$–phase in high pressure die cast materials is reported for Sr/Al-ratios in weight-% above 0.3 [29]. This is in accordance with the XRD patterns of the permanent mould cast alloys AJM51 and AJM52. Mg_2Si is the predominant phase in AS-alloys besides $Mg_{17}Al_{12}$ [30,29]. Both phases are detected in the strontium free alloy ASMX51. In calcium-containing magnesium-aluminium-alloys the formation of the Al_2Ca-phase is reported for Ca/Al-ratios in weight-% above 0.8 [31,32]. In the present case the calcium concentration is too low to result in a sufficient amount of Al-Ca-phase detectable by XRD.

In XRD patterns the peak height of a phase correlates with the according phase fraction in the microstructure [33]. As soon as strontium is added to alloys with 1 % silicon the formation of the $Sr_{6.33}Mg_{16.67}Si_{13}$–phase is observed. With increasing strontium content the height of XRD-peaks for the Mg_2Si-phase continuously decreases, Fig. 5. The Al_4Sr-phase is not detected by XRD as long as Mg_2Si is present. The Sr/Si-ratio of mass fractions in the $Sr_{6.33}Mg_{16.67}Si_{13}$-phase is 1.52 according to stoichiometry. This ratio is only exceeded in case of alloy AJSMX521, 1.98 % strontium, 1.14 % silicon. In this material the Mg_2Si-phase disappears and the Al_4Sr-phase emerges. The $Mg_{17}Sr_2$–phase is not formed though it is reported for Sr/Al-ratios above 0.3 [29,34]. In other words, silicon reacts completely to form $Sr_{6.33}Mg_{16.67}Si_{13}$ as long as sufficient amounts of strontium are available. The excess of strontium in alloy AJSMX521 yields the formation of Al_4Sr. Obviously the ternary compound $Sr_{6.33}Mg_{16.67}Si_{13}$ is formed preferentially instead of Al_4Sr, $Mg_{17}Sr_2$ and Mg_2Si. The $Sr_{6.33}Mg_{16.67}Si_{13}$–phase does not contain aluminium. This means that the strontium content bound in the ternary Zintl-phase can not suppress the formation of $Mg_{17}Al_{12}$. In consequence the formation of the $Mg_{17}Al_{12}$–phase was shown using XRD in all alloys containing 1-wt.-% silicon, see Fig. 5.

Based on the above made assumptions, the phase fractions of the main intermetallic phases formed by strontium, silicon and calcium can be calculated. Tab. 4 shows the results of this calculation. The $Mg_{17}Al_{12}$-phase is not considered as areas supersaturated with aluminium around the $Mg_{17}Al_{12}$-precipitates make it very difficult to estimate the amount of aluminium not bound in the matrix. The amount of strontium not bound in the Al_4Sr-phase was assumed on the basis of results from Pekguleryuz et. al. [34,29]. It was stated that the $Mg_{17}Sr_2$-phase forms above Sr/Al-ratios of mass-% of 0.3. However, it has to be mentioned, that this statement was made for high pressure die cast material.

Tab. 4: Phase fractions of the main phases formed by strontium, silicon and calcium

Alloys	Mg_2Si [Vol.-%]	$Sr_{6.33}Mg_{16.67}Si_{13}$ [Vol.-%]	Al_4Sr [Vol.-%]	$Mg_{17}Sr_2$ [Vol.-%]
AM50	0.05	0.00	0.00	0.00
ASMX51	2.56	0.00	0.00	0.00
AJM50	0.05	0.00	0.30	0.00
ASJMX51	1.90	0.81	0.00	0.00
AJM51	0.05	0.00	1.27	0.00
AJSMX511	0.99	1.28	0.00	0.00
AJM52	0.05	0.00	2.03	2.26
AJSMX521	0.00	2.77	0.34	0.00

Nesper et al. [35] reported the formation of the $Sr_{6.33}Mg_{16.67}Si_{13}$–phase from the three main constituents strontium, magnesium and silicon. Probably the presence of calcium does not influence this phase formation. As its atomic radius is similar to that of strontium, it is likely that calcium atoms substitute for strontium atoms in the $Sr_{6.33}Mg_{16.67}Si_{13}$-phase. The presence of calcium in the phase was shown by EDX measurements for alloy AJMSX50 [22]. The sum of atom fractions for calcium and strontium is in due proportion to the atom fraction of silicon [20,22]. Calcium may completely take over the function of strontium. Nesper et al. [36] reported the formation of Zintl-phase $Ca_7Mg_{7,5\pm\delta}Si_{14}$ from stoichiometric amounts of the elements and the formation of CaMgSi-phase was calculated by Schmid-Fetzer et al. [37] in case calcium is added to AS-alloys.

The addition of alloying elements caused an increase of the tensile yield strength. This may have several reasons. It can be found in literature that certain elements have a grain refining effect on magnesium and magnesium alloys [38,39]. Among those are strontium, silicon and calcium. In fact it is shown in Tab. 3 that the grain diameters were reduced by alloying. Grain refinement according to Hall-Petch equation may be one reason for the increased yield strength. Comparing Tab. 3 and Fig. 7, it can be seen that for alloys AJM51 and AJM52 the grain diameters are reduced compared to AM50 while the yield strength is increased. However, the development of the grain size and the yield strength is not consistent for all alloys. AJMX51 has a yield strength of 56.3 MPa but the grain diameter is bigger than that of alloy AM50. Therefore, another strengthening mechanism should be precipitation hardening due to the higher content of

intermetallic particles in the microstructure.

The reduced elongation at fracture of strontium rich, silicon free alloys like AJM51 and AJM52 is due to the wide spreading morphology of the strontium containing phases Al_4Sr and $Mg_{17}Sr_2$. As can be seen from micrographs Fig. 11 and Fig. 12, cracks grew through the brittle precipitates. In alloys containing strontium and extra silicon cracks are blocked early by the matrix because particles of the $Sr_{6.33}Mg_{16.67}Si_{13}$–phase have a compact shape and lay separate from one another. In Al_4Sr- and especially in $Mg_{17}Sr_2$ precipitates cracks can grow over long distances. Thereby the effective cross section of the tensile test samples is quickly reduced once a crack is formed. The longest crack in Fig. 14 spreads along the Al_4Sr-, not along the $Sr_{6.33}Mg_{16.67}Si_{13}$–precipitate.

The development of minimum creep rates and creep compressions can be explained by the formation of the intermetallic phases. Strontium and calcium incorporate aluminium in form of Al_4Sr-, $Mg_{17}Sr_2$- and Al-Ca precipitates. Thereby the contents of $Mg_{17}Al_{12}$-phase and the accompanying α-matrix, supersaturated with aluminium, are reduced and the creep resistance is improved [17,11]. A decrease of creep rate and creep strain with increasing contents of strontium and calcium is in accordance with the literature [27,32]. Even though silicon does not reduce the content of $Mg_{17}Al_{12}$–phase, it improves the creep resistance of magnesium alloys [40]. According to Dargusch [18] the stabilisation of grain boundaries due to the morphology of Mg_2Si precipitates is responsible for this effect. It can be seen from Fig. 6 that $Sr_{6.33}Mg_{16.67}Si_{13}$ precipitates have a compact shape which would be less suitable for the stabilisation of grain boundaries. From alloy ASMX51 to ASJMX51 and AJSM511 the Mg_2Si-phase is subsequently replaced by $Sr_{6.33}Mg_{16.67}Si_{13}$ and no strontium-containing phases are formed. Tab. 5 compares the volume fractions of the Zintl–phases, the minimum creep rates and the compression strains of the three alloys. The volume fractions of the Zintl–phases were calculated from the chemical compositions, assuming that strontium and silicon form the highest possible amount of the $Sr_{6.33}Mg_{16.67}Si_{13}$–phase. An image-analysis-software was not used due to the very inhomogeneous microstructure of the castings.

Tab. 5: Phase fractions of Zintl-phases and results of compression creep tests at 150°C, 80 MPa, 200 h

Alloy	**Mg_2Si [Vol.-%]**	**$Sr_{6.33}Mg_{16.67}Si_{13}$ [Vol.-%]**	**Mg_2Si + $Sr_{6.33}Mg_{16.67}Si_{13}$ [Vol.-%]**	**Minimum Creep Rate [s^{-1}]**	**Compression [%]**
ASMX51	2.56	0.00	2.56	$1.45*10^{-8} \pm 0.55*10^{-8}$	2.05 ± 0.26
ASJMX51	1.90	0.81	2.71	$1.27*10^{-8} \pm 0.26*10^{-8}$	2.70 ± 0.50
AJSMX511	0.99	1.28	2.17	$1.07*10^{-8} \pm 0.24*10^{-8}$	2.09 ± 0.36

With rising contents of strontium the overall volume fractions of the Zintl-phases remain almost constant or even decrease due to the higher density of 2,675 g/cm^3 for $Sr_{6.33}Mg_{16.67}Si_{13}$ compared to 1.988 g/cm^3 for Mg_2Si. At the same time from alloy ASMX51 to ASJMX51 and AJSM511 the minimum creep rates are reduced and the samples compressions almost remain unchanged. This means that under the given

circumstances, the precipitates of $Sr_{6.33}Mg_{16.67}Si_{13}$ are more effective for the thermal stability than those of Mg_2Si. A clear improvement of the creep resistance is achieved when the $Sr_{6.33}Mg_{16.67}Si_{13}$- and the Al_4Sr–phase are present in alloy AJSMX521.

In general it has to be stated that the permanent mould casting process exhibits relatively low cooling rates. Alloys like AM50 and AJ52 are originally meant to be processed by high pressure die casting. Grain sizes between 0.5 und 10 µm in the casting skin and 20 to 70 µm in the remaining microstructure have been measured for high pressure die cast alloys AM60 and AZ91 [41,42]. Yield strengths between 110 and 160 MPa are reached for high pressure die cast components [13]. Rare earth containing magnesium alloys in the contrary are designed for preparation by the sand- and permanent mould casting process, respectively. By the grain refining effect of zirconium and additionally applied heat treatment yield strengths between 125 and 179 MPa are reached [43]. Magnesium-aluminium alloys may be solution heat treated, as long as the aluminium content is above 6 % [30]. The previous statements demonstrate that the applied permanent mould casting process was suitable to prepare the alloys in the laboratory scale. General impacts of alloying elements and casting process parameters could be detected. However, the process is not the preparation method to reach optimum mechanical properties.

Conclusions

In order to develop a magnesium recycling alloy, strontium, silicon and calcium were added to the high pressure die casting alloy AM50. Eight alloys were prepared by permanent mould casting. The materials phase formation, the properties in the tensile test and the behaviour under compressive creep load were investigated and the results can be summarised as follows.

1. The simultaneous addition of strontium and silicon to magnesium alloy AM50 leads to the formation of the ternary Zintl-phase $Sr_{6.33}Mg_{16.67}Si_{13}$. The phase forms preferably instead of Al_4Sr, $Mg_{17}Sr_2$ and Mg_2Si. Excess strontium leads to the formation of strontium-containing phases like Al_4Sr, excess silicon results in the formation of Mg_2Si.
2. Compared to phases Al_4Sr and $Mg_{17}Sr_2$ the presence of the ternary Zintl-phase has a less detrimental influence on the materials elongation at fracture. The effect can be ascribed to the compact morphology of precipitates from $Sr_{6.33}Mg_{16.67}Si_{13}$.
3. The yield strength increased with addition of the three alloying elements. Grain refinement and precipitation hardening are probable reasons for this development.
4. Strontium, silicon and calcium have a positive influence on the materials creep resistance even when added simultaneously. For the materials creep resistance the ternary Zintl-phase $Sr_{6.33}Mg_{16.67}Si_{13}$ is more effective than the binary Zintl-phase Mg_2Si but less effective than the Al_4Sr- and $Mg_{17}Sr_2$-phase.

The detection of the $Sr_{6.33}Mg_{16.67}Si_{13}$-phase closes a gap in understanding the phase formation of magnesium alloys in general. For recycling the finding is of major importance as knowledge has to be obtained about the interaction of elements not used together in commercial alloy systems.

It has to be decided which amount of alloying elements is reasonable for a proposed recycling alloy. The prepared alloys containing 1% silicon exhibited clearly improved mechanical properties but also a poor castability. Alloys free of silicon, with strontium contents between 1 and 2 % exhibited the highest yield strengths but also the lowest elongations-at-fracture. It can be expected that moderate levels of strontium, silicon and calcium will emerge in automotive scrap fractions. Still magnesium-aluminium alloys like AZ91 and AM50 are predominantly used. To reach high levels of strontium and silicon, extra alloying elements would have to be added during the remelting process. However this would cause additional costs and make the process less attractive. Based on the previous assumptions moderate levels below 1% of strontium and silicon would be reasonable. An Sr/Si-ratio of 1.52 should be aimed for in order to avoid phases like Al_4Sr and Mg_2Si and optimise the materials elongation-at-fracture. Calcium may replace strontium in the $Sr_{6.33}Mg_{16.67}Si_{13}$-phase. Further investigations will focus on the application of the High pressure die casting process and the problem of impurities in scrap fractions.

Acknowledgements

This work was funded by the Helmholtz-Gemeinschaft Deutscher Forschungszentren and the Deutsche Forschungsgemeinschaft within the program 1168 „InnoMagTec“.

References

1. Mineral Commodity Summaries 2009, Magnesium Metal (2009) U. S. Department of Interior, U. S. Geological Survey. http://minerals.usgs.gov/minerals/pubs/mcs/2009/mcs2009.pdf.
2. Mineral Commodity Summaries 2003, Magnesium Metal (2003) U. S. Department of Interior, U. S. Geological Survey. http://minerals.usgs.gov/minerals/pubs/mcs/2003/mcs2003.pdf.
3. Mineral Commodity Summaries 1996, Magnesium Metal (1996) U. S. Department of Interior, U. S. Geological Survey. http://minerals.usgs.gov/minerals/pubs/commodity/magnesium/mgmetmcs96.pdf.
4. Barth A Mg-Application in the 7G-Tronic-Gear. In: 61st Annual World Magnesium Conference, New Orleans, USA, 9.-11. May 2004. International Magnesium Association, p [23]
5. Wolf J, Wagener W The BMW Magnesium-Aluminium Crankcase, a Challenge for State-of-the-Art Light Metal Casting. In: 62nd Annual World Magnesium Conference, Berlin, D, 22.-24. May 2005. International Magnesium Association, p [8]
6. Franke G Industrial Recycling of Magnesium Alloys. In: Ding W (ed) Sinomag Die Casting Magnesium Seminar, Beijing, PRC, 2000. private publisher, pp 237-245
7. Krone K (2000) Aluminiumrecycling. 1 edn. Aluminium-Verlag,
8. Blawert C, Morales E, Kainer KU, Scharf C, Živanović P, Ditze A Development of a New AZ Based Secondary Magnesium Alloy. In: 65th Annual World Magnesium Conference, Warsaw, PL, 18.-20. May 2008. International Magnesium Association, p [8]
9. Blawert C, Fechner D, Höche D, Heitmann V, Dietzel W, Kainer KU, Zivanovic P, Scharf C, Ditze A, Gröbner J, Schmid-Fetzer R (2010) Magnesium Secondary Alloys: Alloy Design for Magnesium Alloys With Improved Tolerance Limits Against Impurities. Corrosion Sci 52 (7):2452–2468. doi:10.1016/j.corsci.2010.03.035
10. Ditze A, Scharf C, Blawert C, Kainer KU, Morales Garza ED (2006) Magnesium Alloy. D Patent WO 2007009435-A1, 25.01.2007
11. Pekguleryuz MO, Baril E Development of Creep Resistant Mg-Al-Sr Alloys. In: Hryn JN (ed) TMS Annual Meeting, New Orleans, USA, Feb 11-15 2001. Minerals, Metals & Materials Soc, pp 119-125
12. Suzuki A, Saddock ND, Riester L, Lara-Curzio E, Jones JW, Pollock TM Effect of Sr Additions on the Microstructure and Mechanical Properties of Mg-Al-Ca Alloys. In: Luo AA, Neelameggham NR, Beals RS (eds) TMS Annual Meeting, San Antonio, USA, Mar 12-16 2006. Minerals, Metals & Materials Soc, pp 523-528
13. ASTM (2007) Standard Specification for Magnesium-Alloy Die Castings. American Society for Testing and Materials,
14. Sato T, Mordike BL, Nie JF, Kral MV An Electron Microscope Study of Intermetallic Phases in AZ91 Alloy Variants. In: Neelameggham N, Kaplan HI, Powell BR (eds) TMS Annual Meeting, San Francisco, USA, Feb 13-17 2005. Minerals, Metals & Materials Soc, pp 435-440
15. Bronfin B, Aghion E, Buch Fv, Schuhmann S, Katzir M (2002) High Strenght Creep Resistant Magnesium Alloys. USA Patent US 7041179-B2, 09.05.2006
16. Waltrip JS Fresh Look at Some Old Magnesium Die Casting Alloys For Elevated Temperature Applications. In: 47th Annual World Magnesium Conference, Cannes, F, May 1990. World Magnesium Association, pp 124-129
17. Dargusch MS, Dunlop GL, Pettersen K Elevated Temperature Creep and Microstructure of Die Cast Mg-Al Alloys. In: Mordike BL, Kainer KU (eds) Magnesium Alloys and Their Applications, Wolfsburg, D, 28.-30. April 1998. Werkstoff-

Informationsgesellschaft mbH, pp 277-282
18. Dargusch MS, Bowles AL, Pettersen K, Bakke P, Dunlop GL (2004) The Effect of Silicon Content on the Microstructure and Creep Behavior in Die-Cast Magnesium AS Alloys. Metall Mater Trans A-Phys Metall Mater Sci 35A (6):1905-1909
19. Fechner D, Blawert C, Hort N, Kainer KU (2009) Recycling of Magnesium Drive Train Components. Sci China Ser E-Technol Sci 52 (1):148-154. doi:10.1007/s11431-008-0288-1
20. Fechner D, Hort N, Kainer KU Magnesium Recycling System Prepared by Permanent Mould- and High Pressure Die Casting. In: Nyberg EA, Agnew SR, Neelameggham MR, Pekguleryuz MO (eds) TMS Annual Meeting, San Francisco, USA, Feb 15-19 2009. Minerals, Metals & Materials Soc, pp 111-116
21. Fechner D, Blawert C, Hort N, Kainer KU Influence of Strontium, Silicon and Calcium Additions on the Properties of the AM50 Alloy. In: Dargusch MS, Keay SM (eds) Light Metals Technology 2009, Gold Coast, Queensland, Australia, 2009. Trans Tech Publications Ltd., pp 459-462
22. Fechner D (2010) Entwicklung einer Magnesium-Recyclinglegierung auf Basis der Legierung AM50. Technische Universtität Clausthal, Clausthal, Germany
23. ASTM (1996) Standard Test Methods for Determining Average Grain Size. American Society for Testing and Materials,
24. DIN (2001) Metallische Werkstoffe Zugversuch. vol 10002-1. Deutsches Institut für Normung e.V. Europäische Norm,
25. DIN (2004) Prüfung Metallischer Werkstoffe - Zugproben. Deutsches Institut für Normung e.V.,
26. ASTM (2005) Standard Practice for Codification of Certain Nonferrous Metals and Alloys, Cast and Wrought. American Society for Testing and Materials,
27. Zhao P, Wang QD, Zhai CQ, Zhu YP (2007) Effects of Strontium and Titanium on the Microstructure, Tensile Properties and Creep Behavior of AM50 Alloys. Materials Science and Engineering A 444 (1-2):318-326. doi:10.1016/j.msea.2006.08.111
28. Liu MP, Wang QD, Zeng XQ, Yuan GY, Zhu YP, Ding WJ Mechanical Properties and Creep Behavior of Mg-Al-Ca Alloys. In: Ke W, Han EH, Han YF, Kainer K, Luo AA (eds) International Conference on Magnesium - Science, Technology and Applications, Beijing, PRC, Sep 20-24 2004. Trans Tech Publications Ltd, pp 763-766
29. Pekguleryuz MO, Kaya AA (2003) Creep Resistant Magnesium Alloys for Powertrain Applications. Adv Eng Mater 5 (12):866-878. doi:10.1002/adem.200300403
30. Avedesian MM, Baker H (eds) (1999) ASM Specialty Handbook - Magnesium and Magnesium Alloys. ASM International - The Materials Informations Society,
31. Ninomiya R, Ojiro T, Kubota K (1995) Improved Heat Resistance of Mg-Al Alloys by the Ca Addition. Acta Metall Mater 43 (2):669-674
32. Sohn KY, Jones JW, Allison JE The Effect of Calcium on Creep and Bolt Load Retention Behavior of Die-Cast AM50 Alloy. In: Kaplan HL, Hryn JN, Clow BB (eds) TMS Annual Meeting, Nashville, USA, Mar 12-16 2000. Minerals, Metals & Materials Soc, pp 271-278
33. Cullity BD (1978) Elements of X-Ray Diffraction. 2 edn. Addison-Wesley Publishing Company Inc.,
34. Pekguleryuz M, Labelle P, Argo D, Baril E Magnesium Diecasting Alloy AJ62X with Superior Creep Resistance, Ductility and Diecastability. In: Kaplan HI (ed) TMS Annual Meeting, San Diego, USA, Mar 02-06 2003. Minerals, Metals & Materials Soc, pp 201-206
35. Nesper R, Wengert S, Zurcher F, Currao A (1999) Electronic Variations in Carbonate- and Phosphane-Related 24- and 26-Electron E-4 Clusters of Silicon and

Germanium. Chem-Eur J 5 (11):3382-3389
36. Nesper R, Currao A, Wengert S (1998) Nonaromatic Planar Si-12 Ring System of Approximate D-6h Symmetry in Ca7Mg7.5 +/-Delta Si14. Chem-Eur J 4 (11):2251-2257
37. Schmid-Fetzer R, Gröbner J Thermodynamic Database for Mg-Alloys: Progress and Application to Mg-Al-Ca-Si Alloy Development. In: Kainer KU (ed) Magnesium Alloys and Their Applications, Wolfsburg, D, 2003. Wiley-VCH, pp 12-17
38. Lee YC, Dahle AK, StJohn DH (2000) The Role of Solute in Grain Refinement of Magnesium. Metallurgical and Materials Transactions A 31 (11):2895-2906
39. StJohn DH, Qian M, Easton MA, Cao P, Hildebrand Z (2005) Grain Refinement of Magnesium Alloys. Metallurgical and Materials Transactions A 36 (7):1669-1679
40. Evangelista E, Spigarelli S, Cabibbo M, Scalabroni C, Lohne O, Ulseth P (2005) Analysis of the Effect of Si Content on the Creep Response of an Mg-5Al-Mn Alloy. Mater Sci Eng A-Struct Mater Prop Microstruct Process 410:62-66. doi:10.1016/j.msea.2005.08.150
41. Bowles AL, Griffiths JR, Davidson CJ Ductility and the Skin Effect in High Pressure Die Cast Mg-Al Alloys. In: Hryn JN (ed) TMS Annual Meeting, New Orleans, USA, Feb 11-15 2001. Minerals, Metals & Materials Soc, pp 161-168
42. Sequeira WP, Dunlop GL, Murray MT Effect of Section Thickness and Microstructure on the Mechanical Properties of High Pressure Die Cast Magnesium Alloy AZ91D. In: Lorimer GW (ed) 3rd International Magnesium Conference, Manchester, GB, Apr 10-12 1996. Inst Materials, pp 63-73
43. ASTM (2007) Standard Specificationd for Magnesium-Alloy Sand Castings. American Society for Testing and Materials,